Available online at www.sciencedirect.com
ScienceDirect
Biochimica et Biophysica Acta 1768 (2007) 228–235
Biochimica et Biophysica Acta
BBA
www.elsevier.com/locate/bbamem

Multilayers at the surface of solutions of exogenous lung surfactant: Direct observation by neutron reflection

D. Follows [a], F. Tiberg [a], R.K. Thomas [a,*], M. Larsson [b]

[a] *Physical and Theoretical Chemistry Laboratory, South Parks Road, Oxford, OX1 3QZ, UK*
[b] *Department of Pediatric Medicine, Lund University Hospital, S-221 85 Lund, Sweden*

Received 11 April 2006; received in revised form 9 October 2006; accepted 11 October 2006
Available online 18 October 2006

Abstract

Pharmacy-grade exogenous lung surfactant preparations of bovine and porcine origin, dispersed in physiological electrolyte solution have been studied. The organization and dynamics at the air/water interface at physiological temperature was analysed by neutron reflection. The results show that a well-defined surface phase is formed, consisting of a multilayer structure of lipid/protein bilayers alternating with aqueous layers, with a repetition period of about 70 Å and correlation depths of 3 to >25 bilayers, depending on electrolyte composition and time. The experimental surfactant concentration of 0.15% (w/w) is far below that used in therapeutic application of exogenous surfactants and it is therefore likely that similar multilayer structures are also formed at the alveolar surface in the clinical situation during surfactant substitution therapy. Lung surfactant preparations in dry form swell in aqueous solution towards a limit of about 60% (w/w) of water, forming a lamellar liquid-crystalline phase above about 34 °C, which disperses into lamellar bodies at higher water concentrations. The lamellar spacings in the surface multilayers at the air/water interface are smaller than those in the saturated limit even though they are in contact with much greater water concentrations. The surface multilayers are laterally disordered in a way that is consistent with fragments of Lα-phase lamellae. The near surface layers of the multilayer structure have a significant protein content (only SP-B and SP-C are present in the preparations). The results demonstrate that a multilayer structure can be formed in exogenous surfactant even at very low concentrations and indicate that multilayers need to be incorporated into present interpretations of *in vitro* studies of similar lung surfactant preparations, which are largely based on monolayer models.
© 2006 Elsevier B.V. All rights reserved.

Keywords: Lung surfactant; Exogenous surfactant; Multilayer structure; Surfactant adsorption; Neutron reflection

1. Introduction

The near zero surface tension of the fluid film lining the alveolar surface is considered to be a prerequisite for breathing, but the underlying molecular mechanism remains an enigma. The alveolar surface is lined by a fluid film, about 0.2 μm thick. The bulk of this film is an aqueous dispersion of so-called lung surfactant consisting of about 90% phospholipid and 10% protein [1]. The phospholipid is unusual in that it has a much higher fraction of the saturated DPPC than exists in other mammalian membranes, more than twice that in mitochondrial membrane, which is the next highest. There are four proteins, called SP-A, SP-B, SP-C and SP-D, of which SP-B and SP-C are distinctly hydrophobic and cationic. The other two are anionic and hydrophilic and are associated into oligomers. Two types of phospholipid aggregates have been observed in lung epithelial fluid, lamellar bodies (LB) and tubular myelin (TM). TM was early identified in electron micrographs as a tubular structure, the bilayer in the cross-section through the tubuli showing a characteristic square pattern with a periodicity of about 500 Å [2]. The LB resemble liposomes with a spacing of around 100 Å.

Numerous studies on lung surfactant function have been reported during the last decades, usually with interpretations based on the monolayer model of the alveolar surface introduced by Clements [3]. During recent years the monolayer model has sometimes been modified, involving a monolayer associated reservoir, e.g. [4–6]. Areas of multilayers in lung surfactant systems have been reported by Schürch et al. [7] and more recently by Alonso et al. [8]. One of us has introduced the concept of an alveolar surfactant surface phase based on

* Corresponding author.
E-mail address: thomas@ermine.ox.ac.uk (R.K. Thomas).

0005-2736/$ - see front matter © 2006 Elsevier B.V. All rights reserved.
doi:10.1016/j.bbamem.2006.10.004

observations of directly deposited alveolar surfactant films by cryo-TEM [9].

In states of disturbed surfactant function, e.g. in the immature lung of a premature infant with inadequate amounts of surfactant, or during surfactant inactivation, e.g. by plasma leakage into the alveolar spaces or in meconium aspiration, respiratory distress syndrome may occur. This life threatening state is known as IRDS (infant respiratory distress) in the neonate. This condition can be cured effectively by the administration of exogenous surfactant.

Exogenous surfactants in clinical use today are so-called natural surfactants, obtained by extraction of lung surfactant from lavaged or homogenized bovine or porcine lungs by organic solvents, which results in a mixture of the bilayer lipids, mainly phospholipids, and two hydrophobic surfactant proteins, SP-B and SP-C. The two hydrophilic proteins in the lung surfactant system, SP-A and SP-D, remain in the water phase and are therefore not present in the final material [10]. Such a lung surfactant extract (LSE) contains only about 1–2% SP-B and SP-C, but is still able to restore adequate physiological function to the surfactant deficient lung in IRDS. The successful therapeutic use of such exogenous surfactant illustrates its powerful functionality and suggests that the functional arrangement in exogenous surfactants may be related to the in-vivo alveolar lining.

Neutron reflection is a technique that is able to probe directly the distribution of amphiphiles along the direction normal to a surface and it is particularly easy to apply to the air/water surface [11]. Ideally, isotopic labeling (hydrogen/deuterium) is used to create the differences in the neutron refractive index needed to highlight different structural features at the surface but there are circumstances where this can be achieved simply by using D_2O instead of H_2O. This substitution is not usually effective for a typical spread monolayer of phospholipid on D_2O because the refractive index of the phospholipid layer approximately matches that of air and the experiment merely sees the roughened interface between the phospholipid monolayer and D_2O. However, if there is any structuring of the phospholipid (or associated protein) in the subphase underneath the monolayer the contrast between phospholipid or protein and D_2O is so high that the experiment becomes extremely sensitive. When the phospholipid protein sample cannot be deuterated, the only circumstance that lead to interesting effects on the neutron reflectivity is therefore when there is sub-surface layering. Lung surfactant and its components are usually explored as spread monolayers (e.g. [12]). The disadvantages of this are that it does not correspond to the in vivo situation and it tends to suppress any tendency of the surfactant to form multilayers. Given these observations and the potential sensitivity of neutron reflection to multilayers we have used the technique to explore the surface structure of solutions of exogenous bovine and porcine lung surfactant.

2. Experimental details

The porcine pulmonary surfactant extract HL-10 is described in [13]. The bovine surfactant used was pharmacy grade Alveofact® produced by Boehringer Ingelheim, Ingelheim, Germany. SP-A was extracted from human alveolar proteinosis patients as described in [14]. Ringer's buffer in D_2O was made up freshly according to the following recipe: 0.1 M NaCl, 0.03 M $NaCH_3CO_2$, 0.004 M KCl, 0.0025 M $CaCl_2$, 0.0001 M $MgCl_2$ and HCl to pH 6. The D_2O was 99.5% isotopically pure from Fluorochem.

The SURF neutron reflectometer at ISIS at the Rutherford Appleton Laboratory, Oxfordshire, UK was used for all the reflectometry measurements [15]. The samples were contained in 20 ml polytetrafluoroethylene sample troughs which were thermostatted at 37 °C and enclosed to prevent contamination of the D_2O by atmospheric water vapour. Measurements were made at four angles of incidence, 0.35, 0.5, 0.8 and 1.5 degrees.

The neutron reflectivity of any layer that is homogeneous in the lateral direction (parallel to the surface) can be modelled *exactly* using the same optical matrix method as used for light and X-rays but using only the equations for polarization perpendicular to the plane of reflection [16]. The scattering length density is directly related to composition through the equation

$$\rho = \sum_i b_i n_1$$

where ρ is the scattering length density, and b_i and n_i are the scattering length and number density of atom i in the layer. The values for b_i are known for nearly all isotopes. Given the above equation and that the *absolute* intensity is measured in a reflectometry experiment, the reflectivity profile gives direct information about both structure and composition along the direction of the surface normal. The normal procedure for analysing an observed profile is to create a model profile with the minimum number of features that will fit the data and use least squares (or some equivalent) to optimize the fit to the observed data. The different methods for doing this in many different circumstances have been reviewed by Lu et al. [17]. In situations where there are repeating layers, such as found for the exogenous surfactant, some sort of quantitative relation between successive repeating layers is generally invoked in order to reduce the number of fitting parameters. An example pertinent to the present work is described in [18].

3. Results

Neutron specular reflectivity profiles were measured for 0.15 wt.% solutions of exogenous porcine lung surfactant in D_2O at 40 °C using four different conditions, each measured over a period of 48 h. The conditions were surfactant with and without added SP-A in Ringer buffer and in unbuffered 0.1 M NaCl plus 0.017 M $CaCl_2$. The samples containing SP-A were made by mixing 60 mg of surfactant with 1 ml of the SP-A solution (1.4 mg/ml) in a syringe for 1 min before adding 2 ml of either the salt solution or Ringer. These samples were then left for 4 h during which time phase separation occurred. The supernatant was removed and dissolved in the appropriate D_2O solution (salt or Ringer). The reflectivities from solutions that had equilibrated for 24 h are shown in Fig. 1.

A selection of data is plotted as a function of momentum transfer $\kappa(=(4\pi\sin\theta)/\lambda)$ where θ is the incident glancing angle and λ is the wavelength of the neutrons) in Fig. 1. For a close-packed phospholipid monolayer excluding water, the reflectivity would be little different from that of D_2O. However, the reflectivity becomes exceedingly sensitive to the presence of any phospholipid immersed in the D_2O in the region of the surface. The profile of D_2O (+ buffer) on its own is shown in both parts of Fig. 1 as small dots with no error bars. The striking features in the profiles of Fig. 1 are that all four different samples show a diffraction peak which is not present in the

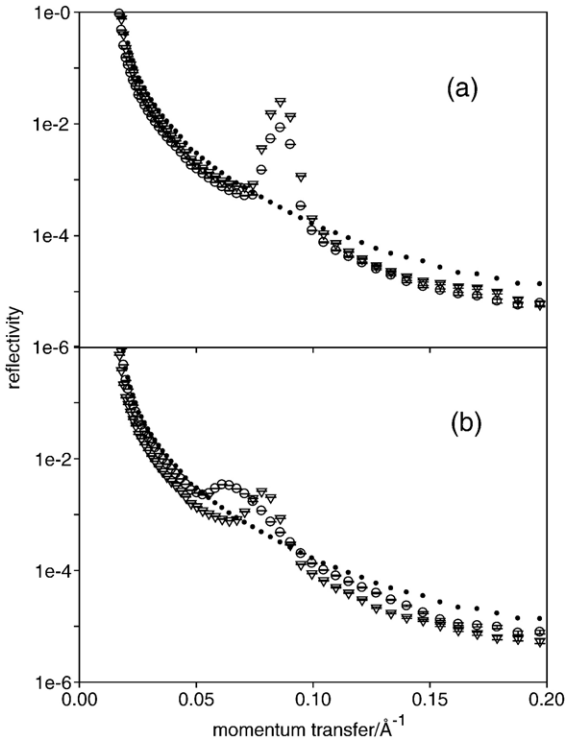

Fig. 1. Neutron reflectivity profiles of the air/water interface of 0.15 wt.% solutions of exogenous porcine surfactant in solutions of (a) unbuffered 0.1 M NaCl plus 0.017 M $CaCl_2$ and (b) Ringer. The dotted lines are the profiles for D_2O solutions with no added surfactant. (○) have added SP-A, (▽ have no added SP-A.

original decaying signal from pure D_2O and that the smoothly decaying parts of the reflectivity drop significantly below that of D_2O buffer. The appearance of the diffraction peak varies between the four solutions, which are 12–24 h old, but becomes well developed after times in the range of hours (sometimes tens of minutes) and always occurs in a similar region. In Fig. 1(a) the sample with SP-A is weaker than the one without SP-A but the situation is reversed in Fig. 1(b). However, it should be realized that the experiment does not allow the simultaneous recording of reflectivity profiles from two different samples and the runs therefore correspond to different ages of surface. Given the geometry of the experiment the diffraction peak can only be caused by some sort of repeating structure underneath the actual surface. Even without a quantitative analysis the shape, position and magnitude of the diffraction peak lead immediately to three important results:

(i) The value of the repeat spacing of the structure (73 ± 0.2 Å in the case of the sample with SP-A and added $CaCl_2$, larger in the case of the Ringer solutions),
(ii) The average number of repeat units in the structure (15 ± 5 in the case of the SP-A/$CaCl_2$ solution with SPA, fewer in the case of the Ringer solutions). This follows from the Scherrer equation for the width of a diffraction peak [19].
(iii) The proportion of water within a repeating unit (40–60% D_2O in the case of the SP-A/$CaCl_2$ solution). This follows because there is a second order peak for the SP-A/$CaCl_2$ sample but it is very weak. For a structure consisting of two blocks of material the second order peak vanishes exactly when the thicknesses of the two blocks are equal, i.e. approximately 50% water.

Fig. 2 shows the reflectivity of a 24-h-old surface of a solution of exogenous bovine surfactant in a 0.1 M NaCl/0.017 M $CaCl_2$ in D_2O. This is directly comparable in terms of conditions to the solution of porcine surfactant in Fig. 1(a) but there are some differences. The repeat spacing is smaller at 68.3 ± 0.2 Å and the narrower diffraction peak indicates that the number of repeat units is greater. Unfortunately, the peak is now narrower than the instrumental resolution and we can only conclude that the average number of repeat units is greater than about 30. Nevertheless, the overall conclusion is that the exogenous bovine surfactant sample also forms multilayers at the air/water interface.

Figs. 1 and 2 show the reflectivities after 12–24 h. The diffraction peaks in these profiles took time to develop and Fig. 3 shows the slow development of the diffraction peak for the porcine surfactant with SP-A in Ringer. The final structure for this sample corresponds to the one with the smallest repeat spacing of 78.8 ± 0.4 Å and the largest average number of repeat units, about 8.

Fig. 1 shows that the development and the final condition of the surface structure depend on electrolyte composition and concentration. Fig. 4(a) shows the development of the diffraction peak for an initially equilibrated surface of porcine surfactant in 0.1 M NaCl to which NaCl has been added to bring the concentration up to 0.17 M and Fig. 4(b) shows the parallel changes for the addition of 0.017 M $CaCl_2$ to an initially equilibrated surface of bovine surfactant in 0.1 M NaCl. In each case there is a very weak diffraction feature at the start of the second addition of electrolyte. After time (only a few minutes in the case of the bovine surfactant) first order and weak second order diffraction peaks develop.

A final important feature of the scattering from the surfaces of these solutions is shown in Fig. 5. The specular reflection profile in this diagram runs horizontally through the center of

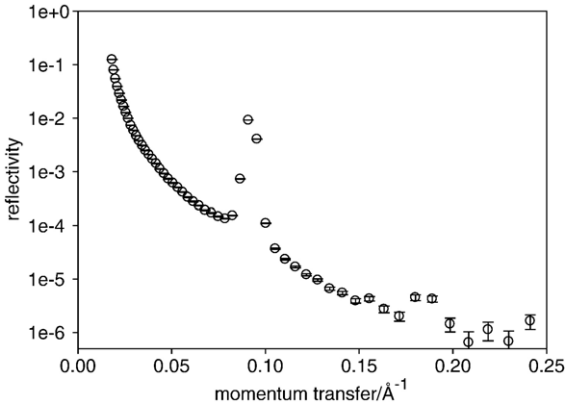

Fig. 2. Neutron reflectivity profiles of a 24-h-old surface of a 0.15 wt.% solution of exogenous bovine surfactant in 0.1 M NaCl/0.017 M $CaCl_2$ solution in D_2O.

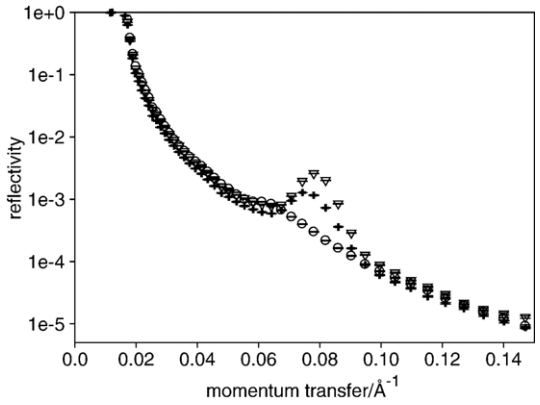

Fig. 3. Neutron reflectivity profiles of a 0.15 wt.% solution of exogenous porcine surfactant with added SP-A in Ringer in D_2O after (○) 6 h, (+) 15 h and (▽) 21 h.

the diagram. Running diagonally across the diagram is a strong streak of off-specular scattering. This is associated with the Bragg diffraction from the multilayered structure and, although there are not good quantitative models for interpreting such scattering at present, the presence of this scattering is direct evidence that the multilayer structure is laterally disordered. This could be because of either roughness or fragmentation of the multilayer. Given the more detailed analysis of the specular reflection presented below, the latter is more likely.

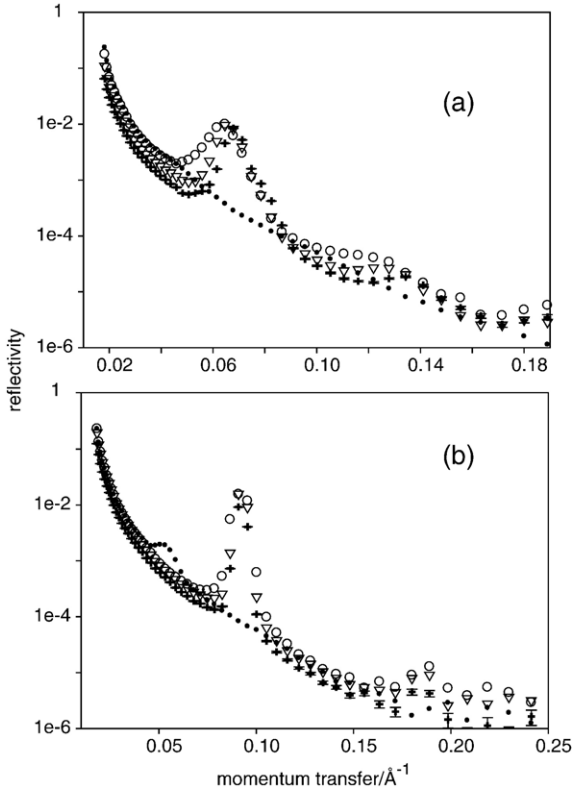

Fig. 4. The evolution with time of the surface of 0.15 wt.% exogenous porcine surfactant and bovine surfactant following addition of further salts without disturbance of the surface. (a) Porcine surfactant equilibrated in 0.1 M NaCl, which was then increased to 0.17 M at time zero: (·) 0 h, (○) 8 h, (▽ 16 h, (+) 27 h. (b) Bovine surfactant equilibrated in 0.1 M NaCl which was then increased by 0.017 M $CaCl_2$: (·) 0 h, (○) 30 min., (▽) 10 h, (+) 20 h.

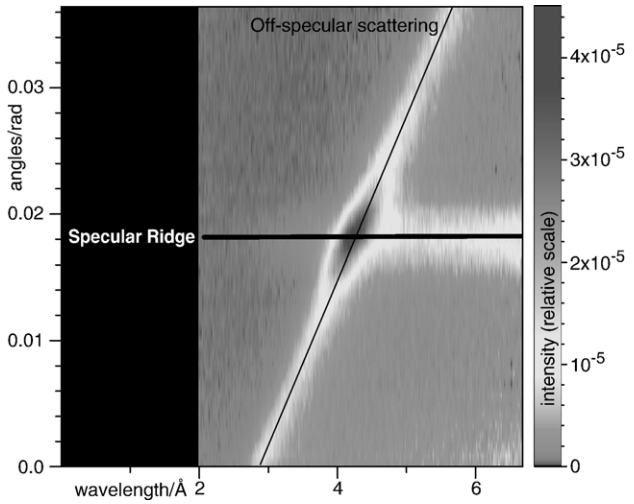

Fig. 5. Off specular neutron scattering from the surface of exogenous porcine surfactant. The solution is the same as in Fig. 1 with Ringer and added SP-A.

4. Discussion

The overall concentration of exogenous surfactant in all the experiments was 0.15% . Taking a phospholipid bilayer to be approximately 30 Å thick the average separation of bilayers in a uniform bulk solution would be about 2000 Å. The presence of multilayers with spacings below 100 Å therefore shows that there is very strong adsorption of exogenous surfactant at the air water interface. It is interesting to compare the spacings we observe with those of Larsson et al. [13] who studied the same porcine surfactant at its swelling limit (about 58% w/w) in aqueous electrolyte solution using X-ray diffraction. With Ringer solution the spacing of the L-alpha phase at 42 °C was 86 Å and that of the gel-phase below the melting transition was 98.5 Å. The corresponding spacings in saline solution were 84 Å and 90.5 Å respectively. These compare with values of 78.8 and 73.0 Å respectively for the surface phase here. The difference in bulk and surface multilayers may reflect a different counter ion distribution in the bulk lamellar phase compared with the surface multilayer phase or it may reflect the uneven distribution of proteins in the surface phase. Accumulation of these proteins at the air interface may affect the spacing of the lamellae. The phase diagram of exogenous surfactant gives a limit of lamellar liquid crystalline phase at about 55–60 w% saline solution [20] at temperatures above about 32–36 °C and a gel phase below this. At higher water concentrations a dispersion of lamellar bodies (fragments of L-α phase) is formed resulting in liposomal particles in the solution. The qualitative conclusions given above do not distinguish between liposomes and unfolded material giving a surface phase of the L-α type. However, the evidence presented below suggests that it is predominantly unfolded material at the surface.

Gulik et al. [21] also used X-rays to study the bulk structure of an aqueous solution of a bovine lung surfactant extract. At 41 °C and about 40% water (the maximum studied) the Lα

phase had a repeat spacing of 74.0 Å which is close to the value we obtain for the porcine surfactant at the surface of salt solution. The differences between the repeat spacings (i) for the porcine and bovine surfactants, (ii) for the porcine surfactant in the presence and absence of SP-A, (iii) for our bovine sample and the different bovine surfactant of Gulik et al., and (iv) for surface and bulk all point to a strong involvement of the proteins in the structure. This is partly because the concentrations of these can be expected to vary according to the extraction protocol and partly because differences are expected between bulk solution and surface. Here we have observed alterations of the lamellar surface structure when SP-A is added. In vivo, SP-A forms tubular myelin structures with the characteristic 500 Å period. The SP-A used in this study, however, is extracted from alveolar proteinosis patients and such SP-A has a slightly different structure [14]. Furthermore, the high water content in the samples would be expected to make any such tubular myelin-like aggregates unstable and fragile. The effects of SP-A on this system requires further studies.

The simple analysis of the data given above leads to the main result that exogenous lung surfactant forms multilayers of some kind at the air/water interface. However, there remain some questions that are not answered by the simple analysis. These questions are (i) whether the diffraction could be from multilamellar vesicles (MLV) in the vicinity of the surface, rather than a genuine surface lamellar phase, (ii) whether the surface is entirely covered with the multilayer, (iii) whether the presence of protein in the layer can be explicitly identified, and if so, where is it in the layer, and (iv) what is the origin of the lateral inhomogeneities in the surface layer? Because reflectivity profiles such as those in Fig. 1 require some technical complexity in their interpretation we discuss the fitting of the data in some detail.

Most authors who have had Bragg peaks in their reflectometry data have used some version of the kinematic theory to avoid the exact optical matrix calculation (see, e.g. [19]). The latter becomes very cumbersome when the number of layers is large. The disadvantage of the kinematic method is that it is less easy to deduce information about the first one or two layers at the surface, although this can be circumvented using an approximation given by Crowley [22]. The first few layers may often be different from the repeating structure that gives rise to the Bragg peak and their contribution can often be observed in the more slowly varying part of the reflectivity away from any peaks. We have analysed the present data using both the kinematic model with the Crowley correction and the full dynamical calculation using the exact optical matrix calculation. The conclusions about all features of the multilayer structure and the first two layers are similar for both methods of analysis. Here we describe only the results from the exact calculation.

The model structure included a repeating structure (which could vary up to 50 bilayers) and two distinct layers at the air surface (two was the minimum required to account adequately for the data). The characteristics of the Bragg diffraction show that there is some sort of decay in the quality of the bilayers with distance from the surface. We used a Gaussian distribution to describe the decay in the amount of phospholipid in each bilayer with an interfacial roughness between each bilayer and water that increased linearly with distance from the surface. Other patterns of decay were tried and all gave similar results. The repeating part of the structure is therefore characterized in terms of five parameters, (i) an average repeat spacing, (ii) the thickness of the water layer in the repeating bilayer structure, (iii) a correlation length in terms of number of layers, (iv) a roughness of the bilayers, and (v) an overall coverage of the available surface by multilayer structure. Parameters (iii) and (iv) are strongly coupled and their nature would vary with the scheme used to describe the decay in order away from the surface. These five parameters determine the width and pattern of the Bragg peaks but make little contribution to the reflectivity between the Bragg peaks except when the correlation drops below about 6 layers. When the correlation length is above this value, it is primarily the near surface structure that determines the remaining shape of the reflectivity profile, particularly the depression of the reflectivity below that of D_2O, which can be seen very clearly in all the profiles on Figs. 1 and 2. This part of the profile is dominated by the two separate surface layers and the parameters that determine this shape are the thicknesses and scattering length densities of these two layers.

We first consider the Bragg peaks. Fig. 6 shows the fits of two sets of data, one with a large number of bilayers comprising the multilayer structure (porcine in Ringer with added $CaCl_2$ but with no SPA) and the other with a small number of bilayers (porcine in Ringer with no SPA). In the added $CaCl_2$ case the width of the peak is accounted for by a correlation about 30 bilayers deep (defined as the bilayer number where the volume fraction of phospholipid has fallen to half its value at the surface). The first part of the distribution used for the best fit is shown in terms of the volume fraction of phospholipid in Fig. 7(a), the remaining space being filled with buffer. For the porcine surfactant in Ringer the correlation length is small and its exact value is sensitive to the choice of decay model, but in terms of the Gaussian distribution is about 3 bilayers. The intensity of the peak in both cases is sensitive to the integrated amount of bilayer in the whole structure and obtaining a fit, even approximate, to both width and intensity of the Bragg peak gives an estimate of how much of the surface is covered by multilayer structure. The coverage of multilayer is between 50 and 60% for the $CaCl_2$ doped sample and between 20 and 30% for the more weakly structured layer. The high intensity of the Bragg peak in the better ordered samples together with the pattern of the off-specular scattering in Fig. 5 indicate that the layer is predominantly L-α phase fragments. The bulk solution at this concentration contains MLV and scattering from MLV in the vicinity of the surface would give rise to a cone of scattering about the incident beam. If there were sufficient intensity from Bragg diffraction from such MLV it would form a cone on the multidetector of a type that we do not observe. If there were a close-packed layer of undistorted MLV adsorbed at the surface these would similarly give a cone of scattering and would be unlikely to give a Bragg peak along a single direction as intense as the one observed (note that the absolute intensity is determined in the reflection experiment). Thus the observed intensity really requires

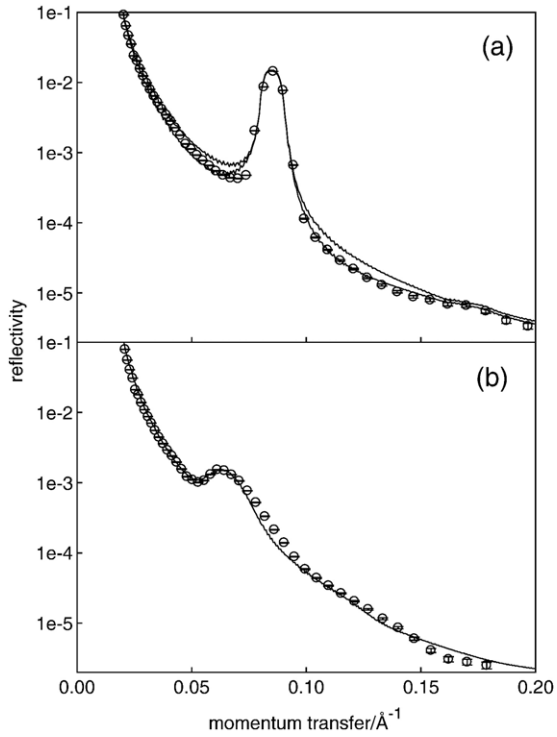

Fig. 6. The fits of a multilayer model to (a) exogenous porcine surfactant in unbuffered 0.1 M NaCl plus 0.017 M $CaCl_2$ and (b) exogenous porcine surfactant, both without SPA. The conditions for the experimental data are as in Fig. 1. The fits in (a) and (b) correspond to the volume fraction profiles of phospholipid shown in Fig. 7(a) and (b) respectively. The two alternative profiles in (a) are calculated for the phospholipid profile shown in Fig. 7(a) and the scattering length density profiles (relative to D_2O) for the two near surface layers shown in Fig. 7(d) and (c) respectively. The upper one of the two corresponds to the structure in Fig. 7(d). The repeat spacings are 74±0.5 and 96±2 Å for (a) and (b) respectively.

reasonably well ordered lamellae. While some of these could arise from highly flattened MLV the probability is that a large fraction have unravelled to give L-α phase fragments. The strong off-specular scattering could arise from defects generated in the unravelling process or from the presence of some remaining MLV walls. Helfrich fluctuations are unlikely to be the origin of the strong off-specular scattering because Helfrich fluctuations will be too small at this bilayer separation. Finally, the presence of only a very weak second order Bragg peak, or complete absence of this peak, is consistent with water and membrane components being of more or less equal thickness in the repeating structure. This result must be regarded as approximate, however, because it is coupled to the disorder parameters for the decay of the multilayer structure, which also tend to suppress this and higher order peaks.

The fitting of the remainder of the reflectivity profile (not the diffraction peak) is also sensitive to the structure of the first layer at the surface, although not in all circumstances. When the Bragg peak is reasonably sharp (bovine and porcine with added calcium), a good fit to the width and height of the Bragg peaks alone is obtained without reference to the first two layers next to the surface. However, if these two layers are taken to be pure phospholipid and pure water respectively, the profile on either side of the Bragg peak is calculated to be far too high as illustrated in one of the calculated profiles in Fig. 6(a). The corresponding scattering length density profile near the surface is shown in Fig. 7(d). This deviation of the reflectivity is exactly as expected because when the two surface layers have this contrast this part of the reflectivity is effectively the reflection from a simple water surface (the scattering length density of a pure DPPC layer is about the same as that of air). As commented on earlier for Figs. 1 and 2, all the reflectivity profiles drop well below that of D_2O and the periodic sub-surface structure does not contribute to the discrepancy. The first layer next to air is expected to be mainly phospholipid (PL) with a thickness in the range 20–30 Å and the second layer should be mainly D_2O with a thickness in the range 30–40 Å. With the two thicknesses constrained in this range it was found necessary to increase the scattering length density of the PL layer and decrease that of the D_2O layer to levels that are inconsistent with the compositions suggested. The best fit of such a structure is also shown in Fig. 6(a) and the corresponding scattering lengths of the two layers are shown in Fig. 7(c). The discrepancies between the two fits are quite large bearing in mind that the plot is on a log scale. The scattering length densities of the two layers are significantly different from those expected from pure PL and D_2O respectively. Attempts to solve the problem by variation of the

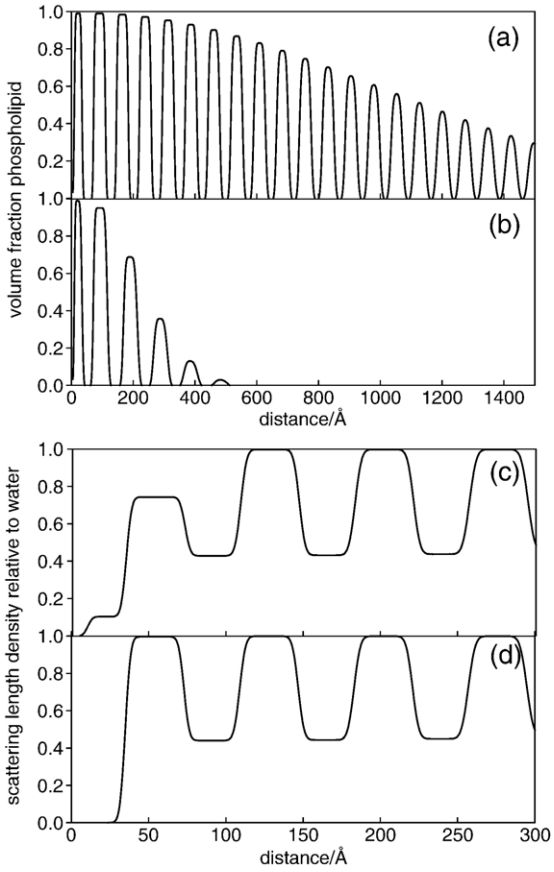

Fig. 7. The structural profiles used for the fits in Fig. 6. (a) and (b) show the multilayer structure (phospholipid volume fraction; the water volume fraction is space filling) used for Fig. 6(a) and (b). (c) and (d) show the surface structures (as scattering length densities relative to D2O) for the two fits in Fig. 6(a) (continuous and dotted lines respectively).

thicknesses of the two layers away from the expected values changes the values of the scattering lengths slightly but does not change the basic effect. The only plausible explanation is that there is a significant amount of protein in both layers. The scattering length density of proteins whose exchangeable H have become D is generally in the range $2–3\times10^{-6}$ Å^{-2}, PL is close to zero and D_2O (with buffer) is about 6.2×10^{-6} Å^{-2}. Taking the scattering length density of protein to be 2×10^{-6} Å^{-2} together with the fitted scattering length densities of about 0.7×10^{-6} Å^{-2} for the nominally PL layer and about 4.7×10^{-6} Å^{-2} for the nominal water layer, these layers contain about 30% and 35% protein respectively. While this is only an approximate calculation, it does indicate that the immediate surface region must contain a significant amount of protein, much higher than the known average protein content (1–2 wt. %). An alternative explanation of the deviations in the scattering length densities of the first two layers is that there is an unusual redistribution of PL and D_2O within the two layers. However, such a redistribution would itself also require a significant amount of protein to be present. Either way, the conclusion is that protein plays an important role in the immediate vicinity of the surface and is present in this region at a much higher concentration than its bulk value (the extracts we have used contain 1–2 wt.% SP-B plus SP-C [23,24]). We can only speculate why there is more protein at the immediate surface. SP-B and SP-C proteins both link up phospholipid bilayers and are extremely surface active on their own. SP-B has four amphiphilic alpha-helical segments which may be partly embedded pairwise in adjacent bilayers, with parallel orientation of the helix axes in relation to the bilayer. SP-C has two palmitic acid chains, assumed to be associated in one bilayer (or monolayer) and one hydrophobic alpha-helical peptide spanning an adjacent bilayer. When the lung surfactant is dispersed in water, some SP-B and SP-C will be tied up in aggregates of phospholipids while some will be in less aggregated form. The DPPC phospholipids will be almost entirely in aggregated form. The high concentration of protein in the first layers may then result from either kinetic or thermodynamic effects. The fastest diffusion to the surface will be the highly surface active SP-B and SP-C, whereas the SP-B and SP-C aggregates with DPPC will diffuse much more slowly. This would result in a high concentration of protein at the surface, which could then be locked into a non-equilibrium state. Alternatively, the hydrophobic protein is thermodynamically essential for linking a highly surface active monolayer of DPPC or protein/DPPC to the lamellar bodies to form the observed multilayer structures. On its own, the lipid forms a monolayer at the surface and it forms lamellar bodies in the bulk, but there is no a priori reason that these should interact, i.e. there is no clear driving force for the formation of multilayers when only lipid is present. There is a parallel for such assisted multilayer formation in solutions of surfactant when very small concentrations of polymer are introduced [25]. The difference here may be that little protein may be necessary to assist multilayer formation once the first two or three surface layers have formed.

The in-vivo efficacy of exogenous surfactant during IRDS is well established. The functional conformation of the exogenous surfactant has been regarded as a monolayer, sometimes with a reservoir of surfactant beneath e.g. [7,8]. The multilayered structure we observe here is not only generated spontaneously and at very low concentrations of surfactant (0.15%) but it both covers a higher proportion of the surface than might be expected for a "reservoir" and is truly part of the surface rather than a sub-surface phase. At concentrations usually employed in exogenous surfactant therapy (5% to 10%) the multilayers could be expected to be even more prominent. The stacks are likely to make the surface region viscous and a higher viscosity would generally reduce the important process of gas transport across the surface. This may be more than compensated by the enhanced solubility of gas in the hydrophobic stacks because the solubility of oxygen is about a factor of ten higher in lipids than in water. Apart from lowering surface tension, a crucial function of lung surfactant is its ability to stabilize the alveolar spaces and minimize damaging shear forces in the lung. The flow properties of lung surfactant multilayers may be fundamental to such protective properties.

Acknowledgements

Marcus Larsson is supported by a Lund University Hospital Grant (ALF). DF was supported by a grant from the EPSRC, UK. HL-10 was kindly provided by LEO-Pharma, Ballerup, Denmark. SP-A was kindly provided by Freek van Iwaarden, Erasmus Medical Center, Rotterdam, The Netherlands.

References

[1] R.H. Notter, Lung Surfactants, Basic Science and Clinical Applications, Marcel Dekker, New York, 2000.
[2] M.C. Williams, Ultrastructure of tubular myelin and lamellar bodies in fast-frozen adult-rat lung, Exp. Lung Res. 4 (1982) 37–46.
[3] J. Perez-Gil, Molecular interactions in pulmonary surfactant films, Biol. Neonate 81 (2002) 6–15.
[4] J.A. Clements, Surface tensions of lung extracts, Proc. Soc. Exp. Biol. Med. 95 (1957) 170–172.
[5] A. Cruz, L.A. Worthman, A. Serrano, C. Casals, K.M.W. Keogh, J. Perez-Gil, Microstructure and dynamic surface properties of surfactant protein SP-B/dipalmitoylphosphatidyl choline interfacial films spread from lipid–protein bilayers, Eur. Biophys. J. 29 (2000) 204–213.
[6] J. Perez-Gil, K.M.W. Keogh, Interfacial properties of surfactant proteins, Biochim. Biophys. Acta 1408 (1998) 203–217.
[7] S. Schürch, F. Green, H. Bachofen, Formation and structure of surface films: captive bubble surfactometry, Biochim. Biophys. Acta 1408 (1998) 180–202.
[8] C. Alonso, T. Alig, J. Yoon, F. Bringezu, H. Warriner, J.A. Zazadzinski, More than a monolayer: relating lung surfactant structure and mechanics to composition, Biophys. J. 87 (2004) 4188–4202.
[9] M. Larsson, K. Larsson, P. Wollmer, Prog. Colloid & Polym. Sci. 120 (2002) 28–34.
[10] R. Pfister, R. Soll, Biol. Neonate 87 (2005) 338–344.
[11] J.R. Lu, R.K. Thomas, J. Penfold, Surfactant layers at the air/water interface: structure and composition, Adv. Colloid Interface Sci. 84 (2000) 143–304.
[12] S.V. Taneva, K.M.W. Keough, Pulmonary surfactant proteins SP-B abd SP-C in spread monolayers at the air–water interface: II. Monolayers of pulmonary surfactant protein SP-C and phospholipids, Biophys. J. 79 (2000) 2010–2023.
[13] M. Larsson, J.J. Haitsma, B. Lachmann, K. Larsson, T. Nylander, P. Wollmer, Enhanced efficacy of porcine lung surfactant extract by

utilization of its aqueous swelling dynamics, Clin. Physiol. Funct. Imaging 22 (2002) 39–48.
[14] J.F. van Iwaarden, F.T. van Berkhout, J.A. Whitsett, R.S. Ooosting, L.M. van Golde, A novel procedure for the rapid isolation of surfactant protein A with retention of its alveolar macrophage stimulating properties, Biochem. J. 309 (1995) 551–555.
[15] J. Penfold, R.M. Richardson, A. Zarbakhsh, J.R.P. Webster, D.G. Bucknall, A.R. Rennie, R.A.L. Jones, T. Cosgrove, R.K. Thomas, J.S. Higgins, P.D.I. Fletcher, E. Dickinson, S.J. Roser, I.A. McLure, R. Hillman, R.W. Richards, E.J. Staples, A.N. Burgess, E.A. Simister, J.W. White, Recent advances in the study of chemical surfaces and interfaces by specular neutron reflection, Chem. Soc., Faraday Trans. 93 (1997) 3899–3917.
[16] J. Lekner, Theory of Reflection, Nijhoff, Dordrecht, 1987.
[17] J.R. Lu, E.M. Lee, R.K. Thomas, The analysis and interpretation of neutron and X-ray specular reflection, Acta Crystallogr., A 52 (1996) 11–41.
[18] J. Schmitt, T. Grunewald, G. Decher, P.S. Pershan, K. Kjaer, M. Losche, Internal structure of layer-by-layer adsorbed polyelectrolyte films—A neutron and X-ray reflectivity study, Macromolecules 26 (1993) 7058–7063.
[19] A. Guinier, X-ray Diffraction, 2nd ed.Freeman, San Francisco, 1963.
[20] M. Larsson, A surface phase model of the alveolar lining: Ultrastructural analysis and in vivo applications. Thesis, Lund University, Sweden, ISBN 91–628–5448–8, 2002.
[21] A. Gulik, P. Tchoreloff, J. Proust, A conformation transition of lung surfactant lipids probably involved in respiration, Biophys. J. 67 (1994) 1107–1112.
[22] T.L. Crowley, A uniform kinematic approximation for neutron reflectivity, Physica, A 195 (1993) 354–374.
[23] D. Häfner, P.G. Germann, D. Hauschke, Effects of rSP-C surfactant on oxygenation and histology in a rat–lung–lavage model of acute lung injury, Am. J. Respir. Crit. Care Med. 158 (1998) 270–278.
[24] W. Bernard, J. Mottaghian, A. Gebert, G.A. Rau, H. von der Hardt, C.F. Poets, Commercial versus native surfactants, Am. J. Respir. Crit. Care Med. 162 (2000) 1524–1533.
[25] D.J.F. Taylor, R.K. Thomas, J. Penfold, The adsorption of oppositely charged polyelectrolyte/surfactant mixtures: neutron reflection from dodecyl trimethyl ammonium bromide and poly(styrene sulfonate) at the air/water interface, Langmuir 18 (2002) 4748–4757.